

Radio and Millimeter Spectral Properties of Newly Identified High Energy Gamma-Ray Sources

S. D. Bloom ^{1,2}

Laboratory for High Energy Astrophysics, NASA/Goddard Space Flight Center,
Greenbelt, MD 20771

J. Hallum

Department of Astronomy, Boston University, 725 Commonwealth Avenue, Boston, MA
02215

H. Teräsranta & M. Tornikoski

Metsähovi Radio Observatory, Metsähovintie 114, FIN-02540 Kylmala, Finland

Received _____; accepted _____

¹NAS/NRC Resident Research Associate, NASA/Goddard Space Flight Center

²Current address: Infrared Processing and Analysis Center, Jet Propulsion Laboratory
and California Institute of Technology, MS 100-22, Pasadena, CA 91125

ABSTRACT

We have conducted a variability study of several radio/millimeter sources which are possible counterparts of high energy gamma-ray sources detected by EGRET. Some sources were possibly variable during this period. The radio source with the highest spectral and temporal coverage, PMN J0850-1213, behaves in a manner consistent with the shocked jet models for extragalactic radio sources proposed in the literature. In addition, GB 105536.5+564424 is an X-ray selected BL Lac object, and if the identification with the EGRET source is correct, it would be the most distant such object detected at energies >100 MeV ($z=0.41$). A future detection in the TeV range as well, could provide an important constraint on absorption of very-high energy gamma-rays by the intergalactic infrared photon field.

Subject headings: BL Lacertae objects: individual (87 GB 105536.5+564424)–galaxies: active–gamma rays: observations–quasars: individual (PMN J0850-1213, PKS 2320-035, 2346+385)

1. Introduction

Though the Energetic Gamma-Ray Telescope (EGRET) on the Compton Gamma Ray Observatory (CGRO) has detected 66 blazars with high confidence (28 with low confidence), and 6 pulsars at energies of 0.1 to 10 GeV, most of the remainder of the sources discovered by EGRET are unidentified with objects at any other wavelength (about 95 in the Second EGRET catalogue and 170 in The Third EGRET Catalogue; Thompson *et al.* 1995; Thompson *et al.* 1996; ; Hartman *et al.* 1998). The unidentified sources fall into two general categories (Özel & Thompson 1996): those which are in the Galactic plane, and those which make up a broader distribution of sources at higher Galactic latitudes. This study has focused on the nature of unidentified EGRET sources at medium to high Galactic latitude ($b > 10^\circ$). In particular, we have considered sources which are likely to be members of the blazar class which were missed in the original identification process. The sources discussed below were labeled as “unidentified” in the Second EGRET Catalog; however, recent observations (largely conducted by the authors) have led to several of these objects being at least “weakly identified” with AGN in the Third EGRET Catalogue. For clarity, we will collectively call all newly identified objects and unidentified objects with possible counterparts, “candidate objects” throughout this paper. Previous analysis (summarized by Mukherjee, Grenier & Thompson 1997; Özel & Thompson 1996) suggests that the medium to high latitude source distribution on the sky is consistent with an isotropic component (presumably blazars) and a second component comprised of at least one Galactic population, possibly related to star formation in the Gould Belt. Though many of these objects may indeed be Galactic, there are several that are likely to be blazars which were missed initially (Zook *et al.* 1997; Bloom *et al.* 1997). Because the first few gamma-ray blazars discovered were very radio bright ($> 1\text{Jy}$ at 5 GHz) and had flat radio spectra, these criteria were subsequently used for identifying high energy gamma-ray sources with blazars. It now seems that this standard may have biased us against sources which

are dim at radio (centimeter) wavelengths, but which are strong millimeter sources. Since there are very few complete and sensitive radio/millimeter surveys between 5 and 90 GHz, it is understandable that such sources would have escaped our attention until recently.

Mattox *et al.* (1997) showed that many of the medium to high latitude unidentified EGRET objects have possible flat spectrum radio source counterparts within their positional confidence contours (“error box”). The evaluation of the *a posteriori* probability that an identification is correct is based on the flux of the source at 5 GHz, spectral index, α , ($F_\nu \propto \nu^{-\alpha}$ here and throughout this paper) and location within the EGRET error box. Both Zook *et al.* (1997) and Bloom *et al.* (1997) closely studied the millimeter and radio spectra of the objects which had the best chances of being correct identifications (and had not previously been accepted as blazar identifications). Zook *et al.* (1997) show that the spectral energy distributions (SEDs or plots of νF_ν) of these candidate objects are different than the composite SED of all of the EGRET blazars (see Figure 1 of the Zook paper). In particular, for a similar level of gamma-ray flux, the radio flux is considerably lower, and the millimeter flux is similar or higher for the candidate objects. These results taken together suggest that the radio spectra of these objects are rising sharply, but that the millimeter spectra are flat, indicative of an intrinsically flat electron spectrum (Hughes *et al.* 1990). To highlight the broad-band properties of the candidate objects in a slightly different manner, we have added the objects observed here (those with potential optical counterparts) to the “color-color” diagram of Comastri *et al.* (1997) (α_{ro} vs. α_{rg} ; Figure 1). They show that the X-ray selected BL Lac objects (or High Frequency Peaked BL Lac objects; abbreviated here as XBL and HBL) show up very distinctly from the flat spectrum radio quasars (FSRQ’s), and the radio selected BL Lac objects (or Low Frequency Peaked objects which we abbreviate as RBL or LBL) fall between on a broad continuum. The upper left corner of this diagram indicates sources with SED’s dominated by gamma-ray emission, whereas the lower left corner have objects which have flatter spectral energy

distributions. As can be seen, by broad band properties alone, the candidate objects of this study fall between the BL Lac objects and the FSRQ's; however, taking the X-ray upper limits into account, it is clear that there is a fairly wide scatter of the candidate objects on this plot. Ghisellini *et al.* 1998 have recently interpreted this progression from XBL's to FSRQ's to represent the increasing dominance of the external Compton mechanism's contribution to the gamma-ray luminosity (with external radiation coming from the broad line region) when going from BL Lac objects to FSRQ's. In this scenario, the gamma-ray spectrum of BL Lac objects would be dominated by synchrotron self-Compton (SSC) emission. Thus, the candidate objects of this study are likely to have no clearly dominant emission mechanism contributing to the observed gamma rays. Though, it is curious that all but one candidate source have gone undetected in X-rays, a part of the spectrum which is likely to have a SSC contribution even when the external Compton model dominates at higher frequencies (Ghisellini *et al.* 1998).

Recently, Laurent-Muehleisen *et al.* (1998; hereafter called LM) have suggested that there is a large class of objects which have broad-band properties between those of RBL's and XBL's. This conclusion was based on a detailed study of AGN which were cross identified in the ROSAT All-Sky and Green Bank Surveys (usually abbreviated as the "RGB" sources). One object which we present in this study, 87GB 105536.5+564424, is also one of the "intermediate" objects in the LM study (and PMN J0459+0600 is an RGB object, but not studied in the LM paper). It is possible that the objects which we are only now identifying with EGRET sources are mostly members of this class.

To more accurately compare the candidate objects with the firmly identified gamma-ray blazars, we have studied their spectral and temporal properties. In the present study we have conducted a three month investigation of the millimeter variability of these candidate objects to determine whether their properties are similar to those of the blazar class. In §2

we discuss our observational procedure at Haystack Observatory. In §3 we summarize the results for the Haystack study, and then focus on 2 particular sources, PMN J0850-1213 , and 87GB 105536.5+564424 which had additional multi-waveband data. In that section we also include predictions for TeV emission from those sources. Our conclusions are then presented in §4.

2. Observations

In addition to the observations summarized previously in Bloom *et al.* 1997, we have observed during 3 sessions at Haystack Observatory in Westford, MA using the 37-meter radio/millimeter antenna. The only successful observations of our program sources were conducted at 43 GHz (22 and 90 were also attempted), and thus we only include the results at that frequency. A drift scan/map method developed by Barvainis *et al.*(1997) to gain sensitivity for observations made within a radome and discussed regarding recent results by Stacy *et al.* (1997) was employed. Typically, we used planets as primary calibrators, especially Mars and Jupiter, but occasionally Venus and Saturn as well. During the period in which the observations were obtained (Jan-Mar 1998), planets were often not available for calibration during much of the night. In such cases, bright quasars such as 3C 273 and 3C279 were used as calibrators. We determined the calibration flux for these objects from the extrapolation of the 22 and 37 GHz spectrum measured at Metsähovi Radio Research Station measured close in time to the date of our observations. If there were no Metsähovi observations during our observations, we interpolated in time between the two closest Metsähovi observations. Variability for these objects on those timescales may account for a about 7% uncertainty in the flux scale. We compared differences in the derived fluxes for sources calibrated against both a planet and a quasar, and these typically agreed to within 5% , about twice as large as the difference in scales derived from two different planets. The

typical statistical measurement uncertainty for weak sources ($3-5 \sigma$) was many times greater than any of these calibration uncertainties. Due to various telescope control glitches (now alleviated with a new pointing computer), we were not able to observe all sources during all three sessions. In addition, a snow storm developed in the late morning of the last session, limiting time and severely limiting the reliability of the observations taken within several hours of the storm. The fluxes of sources observed in the right ascension range of 22 hours to 0 hours are particularly suspect. The results are recorded in Table 1. The identification labels are the primary ones given by NED, so we use these to promote consistency in the literature. However, we note that some of these identifiers use B1950 naming conventions. The column labeled “type” refers to the quality of the identification with an AGN, as defined in Hartman *et al.* (1998). High confidence identifications are labeled with “A”, low confidence id’s are labelled with “a” and possible identifications new to this work are given “?”. The identification for 3EG J0459+0544 differs from that of the Third EGRET Catalogue: they base their positive identification with PKS 0459+06 based on the ~ 1 Jy flux density at 5 GHz ($z=1.106$), and we base our identification on the 43 GHz detection of PMN J0459+0600 which is also a 15th magnitude Palomar Sky Survey source, and has been detected in X-rays by ROSAT (no redshift is known, but if it is similar to the BL Lacs in the LM paper, then the redshift is likely to be < 1). We do not claim that our identification should supersede theirs, just that it should remain a viable candidate. Also, extra care should be taken in noting that these sources have very similar names, and could be confused with each other.

3. Results and Analysis

It seems unlikely that we have observed significant variability for the sources solely observed at Haystack at 43 GHz from January 1998-March 1998. A comparison of the

fluxes (Table 1) shows possible variability for some sources. We apply the simple formula defining a variability parameter, V :

$$V \equiv \frac{F_{max} - F_{min}}{F_{max} + F_{min}} \quad (1)$$

Values of V close to zero show little variability, and values close to one show strong variability, and we consider the variability assessed in this manner to be significant if there is at least a $2\text{-}\sigma$ difference between the error bars of the two data points. Unfortunately, since we only have two data points for each source, a formal probability cannot be assigned to this significance. The value of V for each source is in column (7) of Table 1. In Column (8) we remark on whether this value is significant in the manner we’ve discussed above.

Both PKS 2320-035 and B2349+38 have increased significantly from January into March. However, we note, as we did above, that the weather was particularly bad during the observations of these two sources. Flux increases in both sources are about a factor of 2, after considering the uncertainties. However, the 22 GHz flux for PKS 2320-035 was at the 0.6 level in May (Metsähovi) 1998, two months after the high flux observation at 43 GHz. The 22 GHz flux was on a decreasing trend from the winter. Thus, it seems plausible that the spectrum was relatively flat, and at the 0.7 level in March of 1998. Therefore, a flux increase for PKS 2320-035 should not be ruled out. Of the remaining sources, three are consistent with no variability (The “87 GB” sources in Table 1), and the other three (PMN J0459+0600, PMN J0850-1213, PMN J0619-1140) have shown variability that is less than the $1\text{-}\sigma$ uncertainties of the data.

3.1. PMN J0850-1213

The combined data from several telescopes at different epochs does indeed show variability for some objects. The outburst of PMN J0850-1213 progresses from high to low

frequencies (Figure 2) with little change in the peak flux density. Several months later, the peak flux density drastically decreases as the spectral turnover frequency shifts downward. The observed spectral evolution is consistent with the shocked jet model of Marscher & Gear (1985). After an initial phase in which synchrotron self Compton energy losses dominate the emission spectrum, synchrotron losses, and then adiabatic losses dominate. Since early phases of such flares are expected to produce copious SSC emission (X-ray and Gamma-rays), past gamma-ray detections of this object may be related to flaring events of the type we have seen at lower frequencies. Because of the relatively flat gamma-ray spectral index for this object, we might expect it to be detected at even higher energies. In Figure 3, we plot the SED of this object as well as the extrapolation to TeV energies. In addition, we have plotted the sensitivity of the proposed VERITAS Cerenkov telescope. We have included the expected effects due to intergalactic absorption of very-high energy gamma-rays via pair production with ambient infrared light (Salamon & Stecker 1998). We see that PMN J0850-1213 would easily be detected by VERITAS if its 100 MeV-10 GeV gamma-ray flux and spectral index will be similar in the future. Also, because the source localization of VERITAS is expected to be 18 arcseconds, the identification of the gamma-ray source with the optical/radio source will be much more certain if it is detected in this higher energy range.

It is interesting to note that even in the so-called quiescent state, there are dramatic changes in spectral index between 2 and 37 GHz. This may be caused physically by the same process as in the much stronger outburst, which can be confirmed by monitoring with sensitive VLBA observations simultaneously with the radio flux monitoring. It would also be expected that the optical flux might increase by ~ 0.5 mag (scaling down the ~ 2.0 mag increase preceding the bigger flare) on timescales of a month or so.

In addition, PMN J0850-1213 underwent a weak polarization outburst during the

same period Figure 4). The monthly averaged UMRAO data at 14.5 GHz show that the polarization rose to about 6 ± 1 % in July 1997, about two months after the peak in the total flux density was attained. The polarization percentage had decreased by about a factor of three by the next month, while the total flux density had only decreased (since the peak in May) by a factor of 2. This polarization behavior is qualitatively similar to the stronger outbursts of BL Lacertae described by Hughes *et al.* (1985), and are also due to shock compression in a relativistic jet. As discussed by Marscher (1990), a polarization flare in the Hughes *et al.* (1985) model would correspond to the adiabatic phase of the Marscher & Gear (1985) model. As noted above, the polarization flare occurs in July 1997, which is approximately when the transition to the “adiabatic phase” would be expected to occur.

3.2. 87 GB 105536.5+564424

X-ray selected BL Lac objects detected by EGRET have relatively flat spectral energy distributions over many decades of frequency. 87 GB 105536.5+564424 is similar (Figure 5), and is likely to be the highest redshift X-ray selected BL Lac object detected by EGRET. Interestingly, this [O III] emission line has only been detected once, even though there have been subsequent observations which could have detected it (Marcha *et al.* 1996; Laurent-Muehleisen, S. A. *et al.* 1998). There are two possible factors contributing to the identification and EGRET detection of this object. One is that this source is in back of a low region of hydrogen (HI) column density (within several degrees of the Lockman Hole), making it easier to detect soft X-rays from this object, especially in the less sensitive survey mode (ROSAT All-Sky Survey). In fact, if N_H were $\sim 10^{21}$, the expected ROSAT PSPC count rate would drop by 90 %, and the source would probably not have been detected. It was this X-ray observation that led to the eventual optical identification as a BL Lac object. The other factor, is that there may be a spectral peak (as is evident for Mkn 421 between

10 GeV and 300 GeV; see Macomb *et al.* 1995; Zweerink *et al.* 1997) which is redshifted into the EGRET band, thus resulting in a more favorable EGRET detection.

Several X-ray selected BL Lac objects have been detected by the 10-meter Cherenkov telescope at the Whipple Observatory (Weekes *et al.* 1996). In Figure 5, as above in Figure 3, we compare the extrapolated TeV spectrum of 87GB 105536.5+564424, including absorption effects (Salamon & Stecker 1998), with the sensitivity of the proposed VERITAS telescope. For $\alpha=1.0$, the source would be detected. However, recent analysis provided in the Third EGRET Catalogue Hartman *et al.* 1998 shows that this source has $\alpha = 1.51 \pm 0.27$ in the EGRET range, and thus would likely have a spectral index at least as steep in the TeV range. The source would not be detected if its spectrum is this steep.

4. Conclusions

There is no conclusive evidence that any of the candidate EGRET sources were variable at 43 GHz from Jan 1998–Mar 1998. However, we have clearly shown that at least one flat spectrum radio source within an EGRET source error region (PMN J 0850-1213) has undergone a dramatic multiwaveband flare which could also be related to its detection in high energy gamma-rays. This study shows that monitoring candidate objects within the error regions of EGRET unidentified (or questionably identified) objects could be very fruitful in determining whether the gamma-ray source is related to a blazar. We also suggest future optical spectroscopic observations of radio/millimeter sources with no known redshift (such as PMN J0459+0600) to increase the number of firm identifications with quasars and BL Lac objects. We have also possibly identified the most distant ($z=0.41$) X-ray selected BL Lac object detected by EGRET. Since all prior confirmed TeV detections of XBL's are for objects at $z < 0.1$, any detection of the sources mentioned above (especially with TeV spectra) could be used to test commonly used intergalactic absorption models.

Future ground-based gamma-ray telescopes, such as VERITAS, as well as the spaced based GLAST telescope, will aid in detecting and identifying these sources. In addition, X-ray observations with AXAF and XMM are critical in determining broad band properties of these sources.

5. Acknowledgements

We especially thank Phil Shute, John Ball, and Richard Barvainis for their generous help with the Haystack observations. This research was conducted as part of a NAS/NRC Research Associateship program. In addition, this work was partially supported by the NASA Long Term Space Astrophysics Program while being conducted at the Jet Propulsion Laboratory, California Institute of Technology, operated under contract with NASA.

This research has made use of data from the University of Michigan Radio Astronomy Observatory which is supported by the National Science Foundation and by funds from the University of Michigan.

The Green Bank Interferometer is a facility of the National Science Foundation operated by the NRAO in support of NASA High Energy Astrophysics programs.

REFERENCES

- Barvainis 1998, PASP, 109, 1167
- Bloom et al 1997, Ap J, 488, L23
- Comastri, A. et al. 1997, Ap J, 480, 534
- Ghisellini, G. et al. 1998, MNRAS, 301, 451
- Hartman, R. et al. 1998, Ap J Suppl, in press
- Hughes, P.A., Aller, H. D., Aller, M. F. 1985, Ap J, 298, 301
- Hughes, P. A. et al. 1990, in Parsec Scale Radio Jets, eds. J. A. Zensus & T. J. Pearson
(Cambridge University Press: Cambridge, UK) p. 250
- Laurent-Muehleisen, S. A. 1998 Ap J S, 118, 127
- Macomb, D. J. et al. 1995, Ap J, 449,L99
- Marscher, A. P. 1990, in Parsec Scale Radio Jets,eds. J . A. Zensus & T. J. Pearson
(Cambridge University Press: Cambridge, UK) p. 236
- Marcha, M. J. M. et al. 1996, MNRAS, 281, 425
- Marscher, A. P. 1977, ApJ, 216, 244
- Marscher, A. P., & Gear, W. K. 1985, ApJ, 298, 114
- Mattox, J. R. et al 1997, Ap J, 481, 95
- Mukherjee, R., Grenier, I., & Thompson, D. J. 1997, in Proceedings of the Fourth Compton
Symposium, eds. C. D. Dermer, M. S. Strickman, & J. D. Kurfess (AIP: Woodbury,
NY) p. 394

- Ozel, M. E. & Thompson, D. J. 1996, Ap J, 463, 105
- Salamon, M. H., & Stecker, F. W. 1998, Ap J, 493, 547
- Stacy, J. G., et al. 1997, in Proceedings of the Fourth Compton Symposium, eds. C. D. Dermer, M. S. Strickman, & J. D. Kurfess (AIP: Woodbury, NY) p. 1442
- Thompson, D. J. , et al. 1995. ApJS, 101, 259
- Thompson, D. J. , et al. 1996, ApJS, 107, 227
- Weekes, T. C. , et al. 1996, A &AS, 120, 603
- Zook et. al. 1997, AJ, 114, 1121
- Zweerink et al. 1998, Ap J, 490, L141

FIGURE CAPTIONS

Fig. 1.— Plot of radio/optical spectral index vs. X-ray/ gamma-ray spectral index for firmly identified blazars and candidate sources. The filled circles are quasars, open squares are bl lac objects and the candidate identifications are asterisks

Fig. 2.— Spectral evolution of PMN J0850-1213

Fig. 3.— The spectral energy distribution of PMN J0850-1213. The extrapolation to higher energies (with absorption effects included) is added.

Fig. 4.— The polarization fraction of PMN J0850-1213 during the 1997 flare

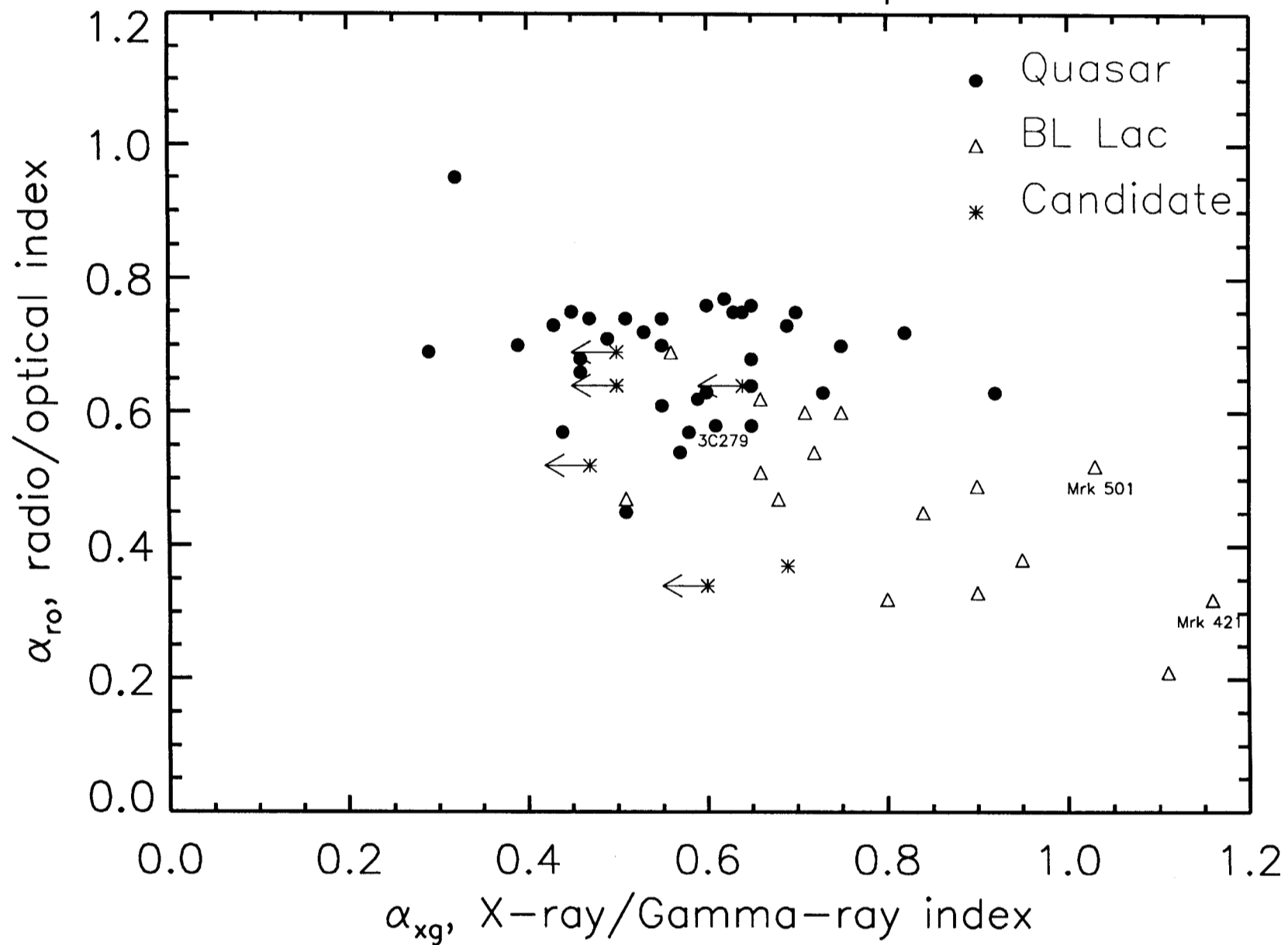
Fig. 5.— Similar to Figure 3, except for B 1055+5644

TABLE 1
43 GHz OBSERVATIONS AT HAYSTACK OBSERVATORY

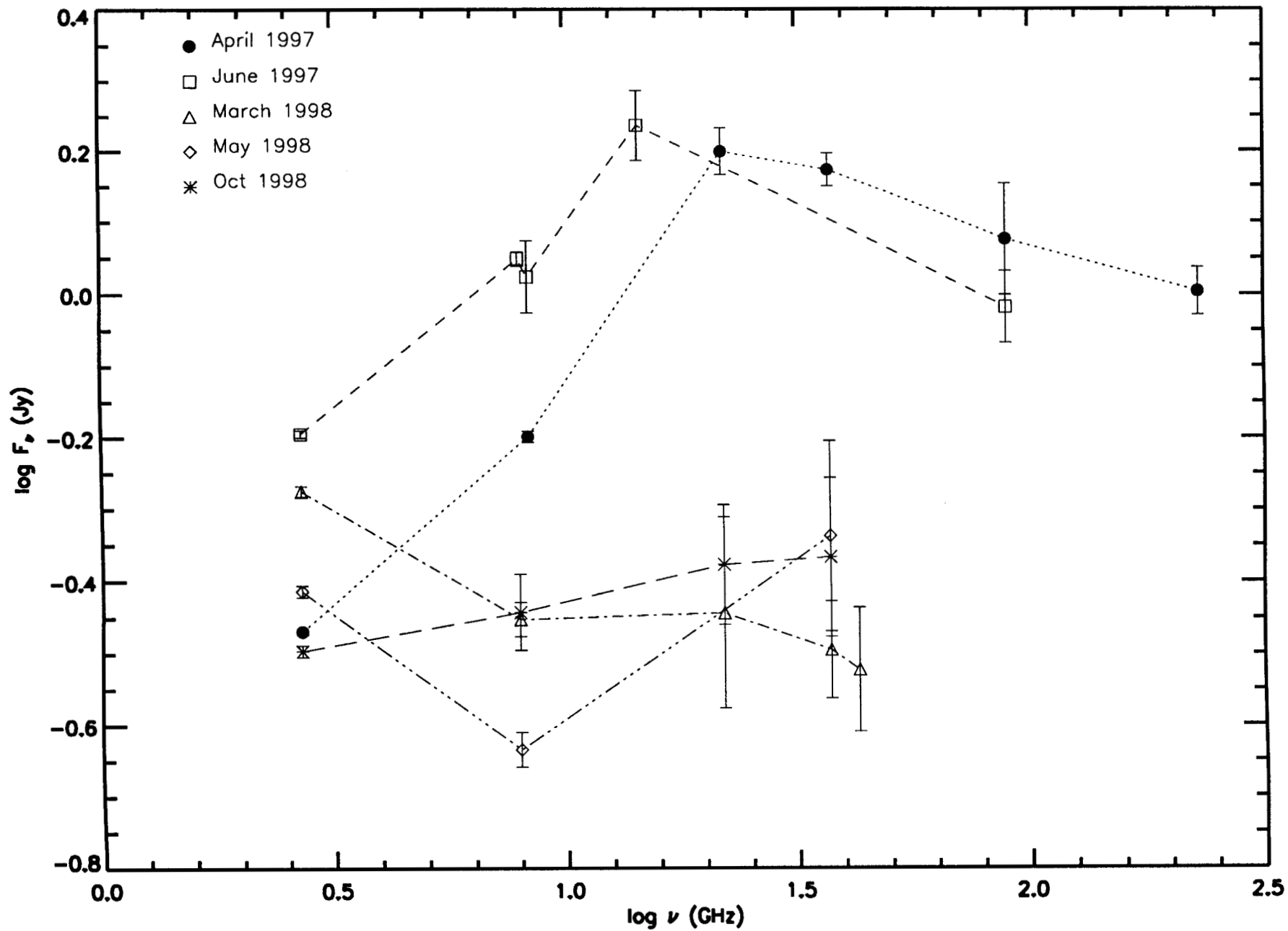
EGRET Source (1)	Identification (2)	Type (3)	Jan 1998 (4)	Feb 1998 (5)	Mar 1998 (6)	V (7)	Variable? ^a (8)
3EG J0459+0544	PMN J0459+0600	?	...	0.29 ± 0.03	0.50 ± 0.15	0.27	No
3EG J0622-1139	PMN J0619-1140	A	...	0.26 ± 0.03	0.18 ± 0.04	0.18	No
3EG J0743+5447	87 GB 073840.5+543188	A	0.20 ± 0.13	...	0.20 ± 0.05	0.00	No
3EG J0852-1216	PMN J0850-1213	A	...	0.19 ± 0.03	0.30 ± 0.07	0.22	No
3EG J1052+5718	87 GB 105536.5+564424	a	0.17 ± 0.04	...	0.15 ± 0.03	0.06	No
3EG J1236+0457	MG J123931+0443	a	0.31 ± 0.04	...	0.24 ± 0.05	0.13	No
3EG J2321-0328	PKS 2320-035	A	0.27 ± 0.06	...	0.80 ± 0.17	0.50	Yes
3EG J2352+3752	2346+385	a	0.17 ± 0.05	...	0.70 ± 0.20	0.61	Yes

$$^a V \equiv \frac{F_{\max} - F_{\min}}{F_{\max} + F_{\min}}$$

Correlation of Broadband Spectral Indices



PMN J0850-1213 SPECTRUM



22.1

SED OF PMN J0850-1213 ($z=0.56$; 2EG J0852-123)

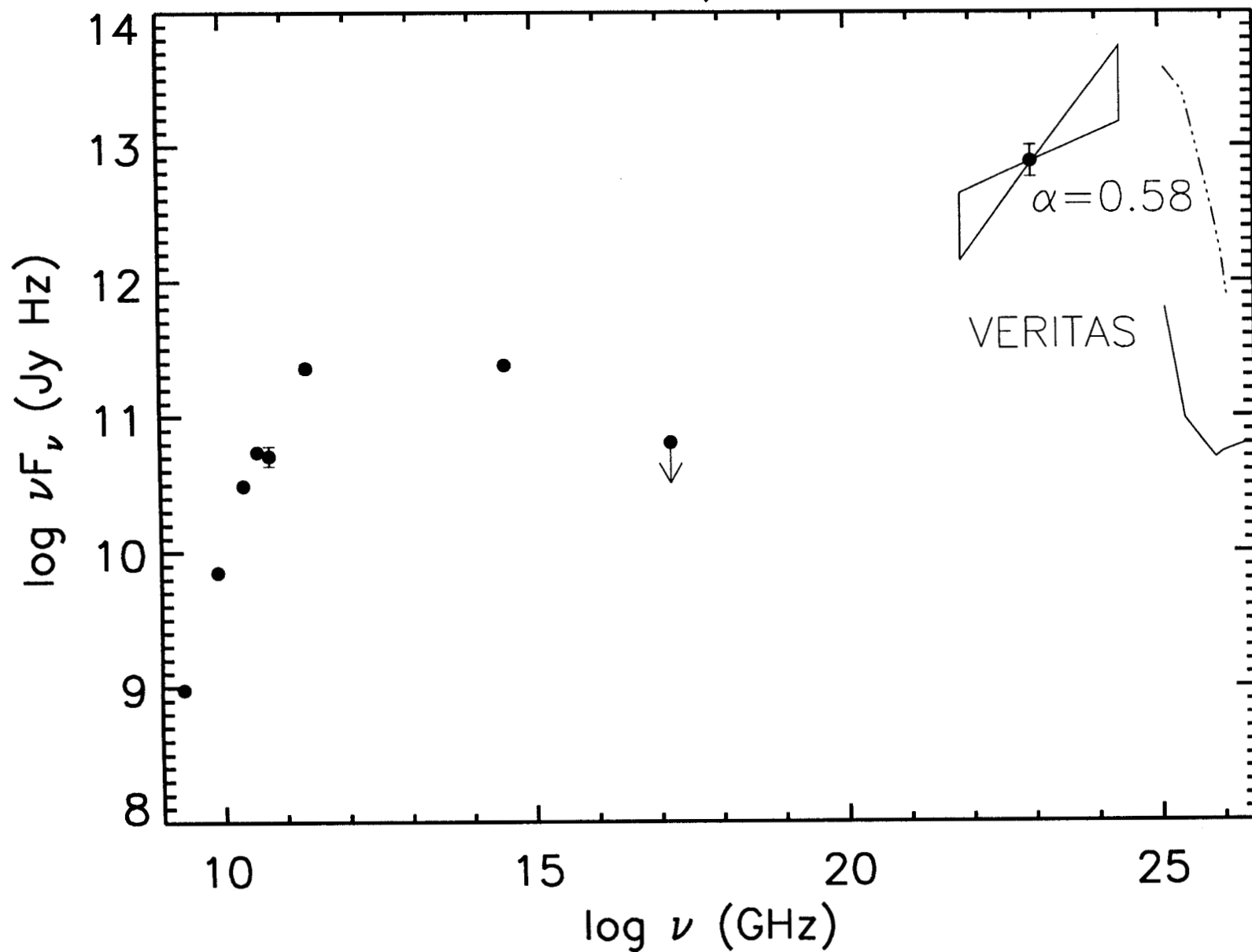
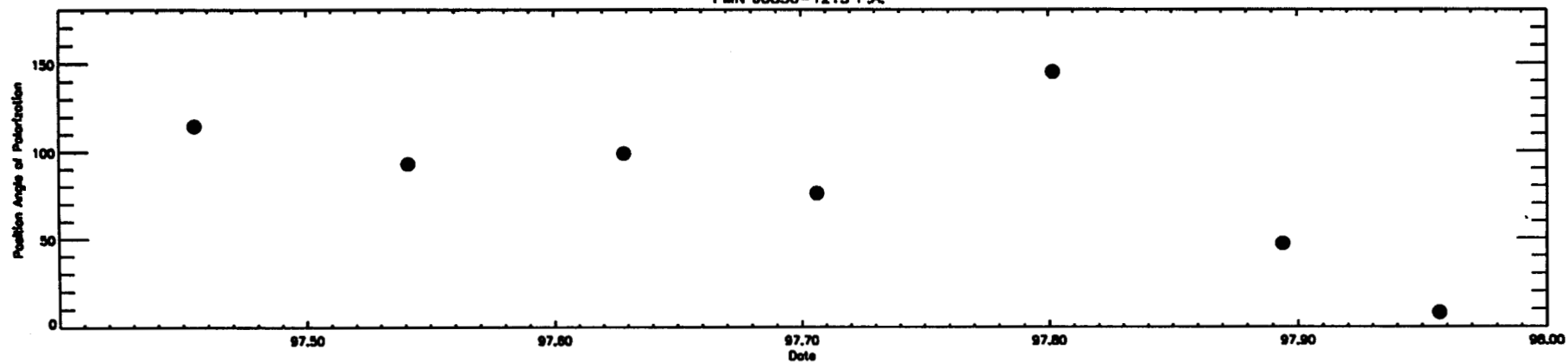
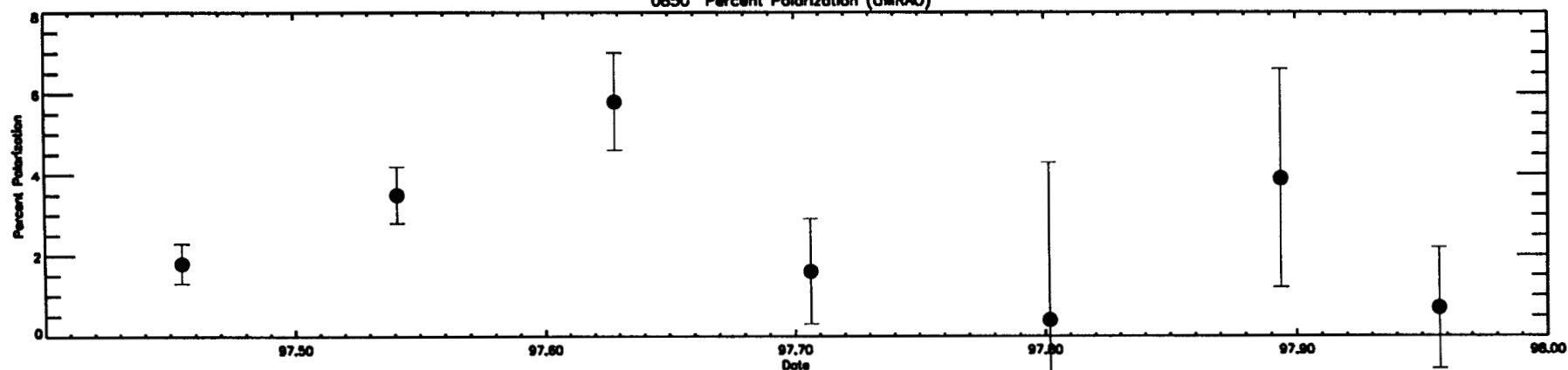


Fig. 3

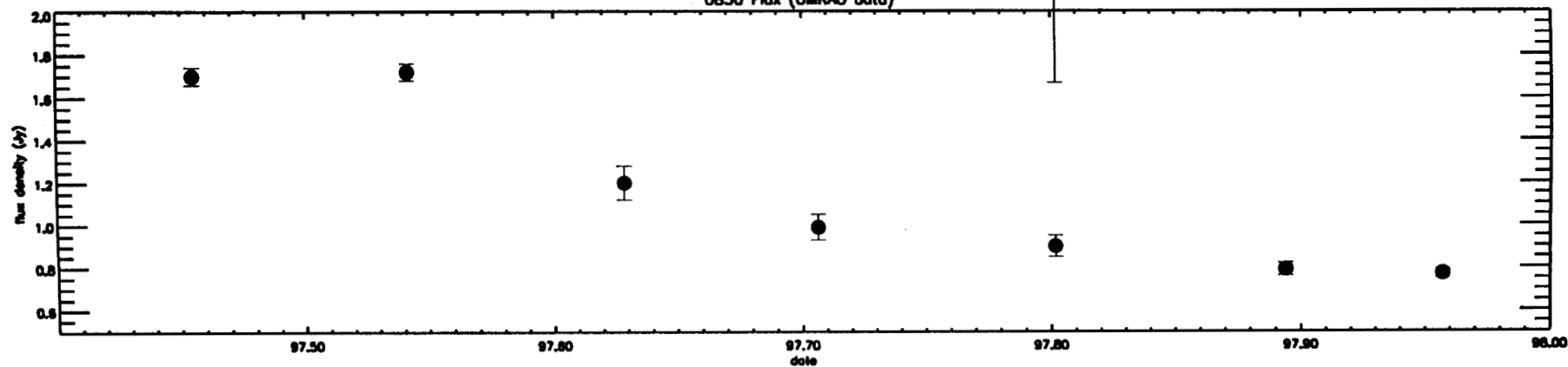
PMN J0850-1213 P.A.



0850 Percent Polarization (UMRAO)



0850 Flux (UMRAO data)



SED of B1055+5644 ($z=0.41$; 2EG J1054+5736)

